The Effects of Thermooxidative Aging on the Fatigue Behavior of a Structural Adhesive

FRED J. WEBER,* ROBERT E. MONTGOMERY, J. SCOTT THORNTON, and DAVID F. WHITE, *Texas Research Institute, Inc., Austin, Texas 78746*

Synopsis

The kinetics of autoxidation of FM-73U, a rubber-modified epoxy adhesive, were investigated by Fourier transform infrared analysis. Absorbance spectra for thin samples aged in hot, moist, oxygen-rich environments were used to assess a plausible reaction mechanism; rate constants, Arrhenius plots, and oxidation rates were determined. Concurrently, crack growth rates were measured on specimens which had been exposed to similar environments for periods of up to 8 months. Paris parameters measured in these tests were correlated with the results of the oxidation studies. These correlations were used to predict the crack growth rate of the adhesive after 10 years of aging in ambient conditions. Although the prediction indicates that the adhesive becomes more brittle with age, the changes are not severe.

INTRODUCTION

The rate of cyclic crack growth in a structural adhesive is an important factor governing the lifetime of a bonded joint. Current methods for characterizing the cyclic crack growth rates of freshly prepared (unaged) polymeric materials are usually based on a variation of the Paris law,[1] which relates the incremental crack growth per load cycle to the stress intensity at the crack tip or to variables associated with energy changes occurring during crack growth. In its simplest version the Paris law may be written as

$$da/dN = C(\Delta K)^{\gamma} \tag{1}$$

where da/dN is the incremental crack growth per cycle and ΔK is the difference between the maximum and minimum stress intensity factor at the crack tip. C and γ are material parameters.

Paris' type relationships were developed first for metals and are presently being applied to polymers.[2] As yet, there is no systematic way of calculating the Paris parameters from first principles and fundamental material properties. Instead, the Paris parameters are evaluated empirically for each material by performing crack growth experiments on representative specimens exposed to appropriate environments. This approach serves well insofar as aging effects are not a concern. However, the combined effects of time, temperature, oxidation, hydrolysis, and physical aging may lead to pronounced changes in the Paris parameters, especially for polymeric ma-

* Present address: Thermon, Inc., San Marcos, Texas 78666.

Journal of Applied Polymer Science, Vol. 29, 3499–3511 (1984)
 CCC 0021-8995/84/113499-13$04.00

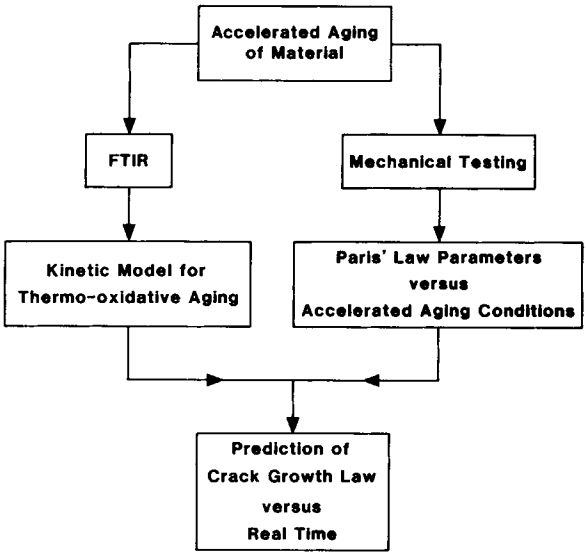

Fig. 1. Diagram of experimental plan.

terials. Thus, methods for characterizing the cyclic fatigue properties of polymers over long service lifetimes need to be developed.

Fortunately, powerful analytic tools capable for tracking structural changes at the molecular level are becoming available. These have lead to a better understanding of polymer degradation kinetics, raising the possibility that physicomechanical changes which occur over a lifetime of service can be predicted. This report presents an attempt to predict changes in the fatigue characteristics of FM-73U (a product of the American Cyanamid Corp.), a rubber-modified epoxy which is under consideration as an adhesive for the bonding of primary structures in aircraft. Autoxidation is thought to be the dominant aging mechanism in this material. Fourier transform infrared analysis (FTIR) was used to develop a kinetic model for the autoxidation of this material. Oxidation rates obtained from the model were correlated with Paris law parameters (obtained on accelerated aged specimens) to predict crack growth rates over a 10-year period. Figure 1 presents the framework of this approach. The environments used to accelerate the aging of FM-73U are summarized in Tables I and II.

KINETIC MODEL FOR THERMAL OXIDATION OF FM-73U

Oxidation of a thermosetting resin is an irreversible aging process that can affect the response, fracture, and fatigue behaviors of the material. It has been observed in FM-73U under warm, moist conditions.[3] Katz and Buchman[4] demonstrated the deleterious effects of oxidation on the dynamic mechanical properties of diamine cured epoxy resins in specimens aged at elevated temperatures in air.

Numerous studies have established that the thermal autoxidation of elastomers is a radical chain reaction. The primary intermediates are hydroperoxides which proceed rapidly through a series of radical propagation

TABLE I
Aging Environments for Cyclic Crack Growth Specimens[a]

Temperature (°C)	Relative humidity (%) at 50°C				Relative humidity (%) at 60°C			
	0		90		0		90	
O_2 partial pressure ratio (P_{ox}/atm)	0.40	1.00	0.40	1.00	0.40	1.00	0.40	1.00

[a] Half were tested after 18 weeks of aging; the remainder were tested after 8 months of aging.

actions to eventually produce carbonyl containing compounds such as aldehydes, ketones, esters, and lactones.[5] Similar studies of epoxy resin systems have resulted in the same general conclusions,[6] suggesting that the following mechanisms play a role in the oxidation of FM-73U:

(1) Oxygen and the polymer combine to form peroxidic or hydroperoxidic species.

(2) Peroxides and hydroperoxides decompose to form free radicals.

(3) Radicals propagate to form a variety of active intermediates.

(4) Termination results in the formation of at least one molecule of a carbonyl containing species per radical termination reaction.

A kinetic model for thermal oxidation in FM-73U was developed from the results of a preliminary experiment in which a thin film of FM-73U was exposed to an oxidizing atmosphere at elevated temperature. The characteristics of the oxidation process were monitored by comparing FTIR spectra obtained after successively longer exposure times with the spectrum of the as-molded, unaged material. Absorbances corresponding to ν(O—H) at 3314 cm^{-1}, ν(C=O) at 1727 cm^{-1}, and ν(C—O) at 1057 cm^{-1} increased with aging time while decreases were observed for ν(C—H) in methyl groups at 2965 cm^{-1}. These observations suggest the following free radical model:

Initiation:

$$\text{polymer} \xrightarrow{k_i} \text{radicals, frequently} \begin{cases} \text{Poly–OOH} \longrightarrow \text{Poly–O}\cdot + \cdot\text{OH} \\ \text{or} \\ \text{Poly–H} \longrightarrow \text{Poly}\cdot + \text{H}\cdot \end{cases} \tag{2}$$

Propagation:

$$\begin{aligned} &\text{Poly–O}\cdot + \text{Poly–H} \xrightarrow{k_1} \text{Poly–OH} + \text{Poly}\cdot \\ &\cdot\text{OH} + \text{Poly–H} \xrightarrow{k_1} \text{H}_2\text{O} + \text{Poly}\cdot \\ &\text{Poly}\cdot + \text{O}_2 \xrightarrow{k_2} \text{Poly–O}_2\cdot \text{ (alkyl peroxy radical)} \\ &\text{Poly–O}_2\cdot + \text{Poly–H} \xrightarrow{k_3} \text{Poly–O}_2\text{H} + \text{Poly}\cdot \end{aligned} \tag{3}$$

Termination:

$$2\ \text{Poly–O}_2\cdot \xrightarrow{k_t} \underset{\diagup\ \diagdown}{\overset{\overset{\text{O}}{\|}}{\text{C}}} \text{ containing products} + \text{O}_2 \tag{4}$$

If we assume that homogeneous decompositions of Poly-OOH into Poly-O · and -HO · require more thermal energy than is available at 60°C or below, then the primary consumer of Poly-H will be the abstraction reaction governed by k_3.[7]

This radical mechanism allows derivation of a rate equation for the oxidation process. If it is assumed that steady-state conditions exist in the polymeric alkyl peroxy radical Poly-O_2 ·, then

$$k_2[\text{Poly} \cdot]\,[O_2] = k_3][\text{Poly-}O_2 \cdot][\text{Poly-H}] + k_t[\text{Poly-}O_2 \cdot]^2, \quad (5)$$

i.e., the rate of production of Poly-O_2 · equals the rate of consumption of Poly-O_2 ·. Note that the left-hand side of eq. (5) represents the rate of the only reaction in the entire mechanistic sequence which consumes an appreciable quantity of oxygen. Therefore, $k_2[\text{Poly} \cdot][O_2]$ = rate of oxidation, ρ_{ox}.

An extensive FTIR program was undertaken to monitor changes in the molecular composition of FM-73U as function of exposure time, temperature, relative humidity, and oxygen partial pressure. The measured concentrations were subsequently used to evaluate the rate constants and Arrhenius parameters associated with the steady-state oxidation model.

FTIR SPECIMEN PREPARATION AND EXPOSURE HISTORIES

Films of FM-73U approximately 0.025–0.05 mm thick were prepared in a laboratory press by molding two piles of material between polished aluminum plates. Specimens were cured using the manufacturer's suggested schedule of 1 h at 121°C. This procedure produced 10 × 15 cm (4 × 6 in.) sheets of material which were checked for thickness and then cut into smaller 5 × 6.3 cm rectangular specimens. These specimens were secured between the cover plates of a specially designed plexiglass IR sample cell and aged in the environments specified in Table II.

FTIR SPECTRAL ACQUISITION AND ANALYSIS

Absorbance spectra, similar to the zero time spectrum shown in Figure 2, were taken on a Nicolet 7199 instrument after each aging interval. The interval lengths varied from 2–3 days to as long as 8 months, depending on the approximate rates of change observed in the initial stages of oxi-

TABLE II
Aging Environments for Specimens Used in the FTIR Oxidation Studies

Temp (°C)	Relative humidity (%)	O_2 partial pressure ratio (P_{ox}/atm)
40	89	0.20, 0.40, 1.00
40	0	0.20, 0.40, 1.00
50	84	0.20, 0.40, 1.00
50	0	0.20, 0.40, 1.00
60	84	0.20, 0.40, 1.00
60	0	0.20, 0.40, 1.00

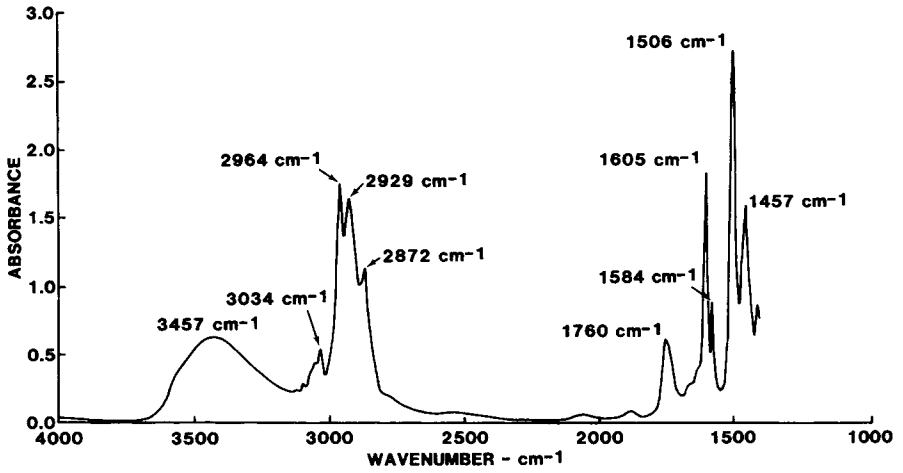

Fig. 2. FTIR absorbance spectrum of unaged FM-73U.

dation. Each spectrum was digitized and stored for future processing. The peak assignments for the zero time spectrum are listed in Table III.

A representative difference spectrum for specimens aged in dry environments is shown in Figure 3. The dry specimens exhibited a gradual growth, with time, of the absorbance in the vicinity of 3297 cm^{-1}. This growth is indicative of hydroperoxide (ROOH) and alcohol (R—OH) group formation. The negative absorbances at 2929 cm^{-1} and around 2872 cm^{-1} correspond to loss of (C—H) moieties in $—CH_2—$ and $—CH_3$. The (O—H) absorbance at

TABLE III
IR Peak Assignments for Unaged Specimens of FM-73U

Absorbance frequency (cm^{-1})	Absorbing functional group	Probable moiety
3457	ν(O—H)	Poly-OH
3034	ν(C—H)	Ar—H
2964	ν(C—H)	$R—CH_3$
2929	ν(C—H)	$R—CH_2—R'$
2872	ν(C—H)	$R—CH_3$
1760	ν(C=O)	ROOR'
		Ester
1667	ν(R—O)	Ar—O
1605	ν(C=C)	Ar } Quadrant
1584	ν(C=C)	Ar } stretch
1506	ν(C=C)	Ar }
1457	ν(C—C)	Ar
1414		
1384	δ(C—H)	$Ar—C(^{\bullet}Me)_2—Ar$
1362	δ(C—H)	
1240	ν(C—O—C)	Ar—O—R
1186	ν(C—C)	Ar—C(C)—Ar

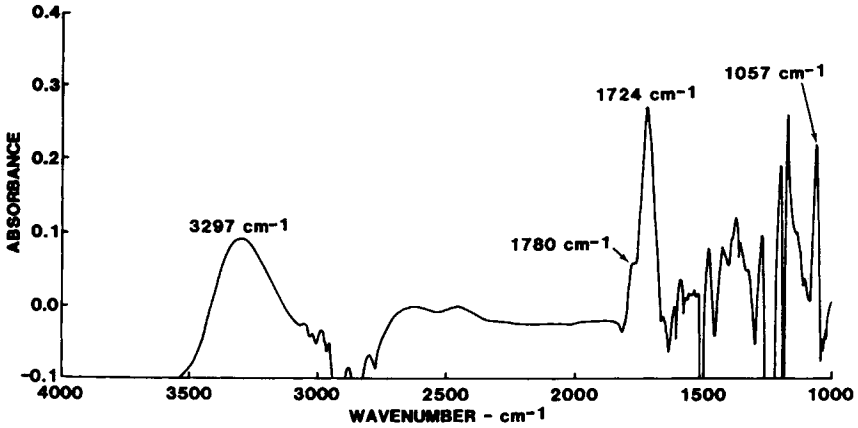

Fig. 3. FTIR difference spectrum for FM-73U aged for 3833 h at 60°C in a 20% oxygen, 0% relative humidity environment.

3457 cm^{-1} in Figure 2 shifts to lower frequencies with aging. This suggests a lengthening of the (O—H) bond due to increased polarity within the material. The pronounced growth in absorbance in the region between 1820 cm^{-1} and 1654 cm^{-1} is caused by formation of several carbonyl containing products which have previously been identified by Lin et al.[6] The shoulder at approximately 1780 cm^{-1} is due to perester or peracid groups while the peak at 1724–1730 cm^{-1} is due to formation of aldehyde and ester moieties. Aliphatic ethers, (R—O—R), are the most likely source of the increasing absorbance seen at 1057 cm^{-1}.

The spectra for the moist specimens exhibited the same features as the dry specimens with the addition of a low shoulder near 3600 cm^{-1}, corresponding to (O—H) absorbances caused by the additional sorbed moisture.

Validation of the oxidation model requires a determination of concentrations of (Poly-H) and (C=O) from the spectra. Concentrations were determined from absorbances via Beer's law. Calibrations of the (C=O) and (C—H) molar absorbances were made using the spectra of standard solutions of propionaldehyde, which exhibits a (C=O) peak at 1732 cm^{-1} and *n*-nonane, which exhibits four discrete (C—H) absorbances between 3000 cm^{-1} and 2800 cm^{-1}.

The concentrations of (C=O) and (C—H) in the aged FM-73U specimens were then determined as a function of exposure time by

(1) integrating the baseline absorbance spectrum over the (C=O) and (C—H) absorbance regions,

(2) integrating the difference spectra of specimens aged for various times,

(3) forming sums of integrated absorbances to determine total integrated absorbance as a function of times, and

(4) calculating concentrations of (C=O) and (C—H) from Beer's law and the calibration values of the molar absorbances.

According to the steady-state rate equation (5), the rate of oxidation is equal to the sum of the rates of a reaction in which (Poly-H) is consumed and a reaction in which two polymeric radicals terminate with each other.

The rate of consumption of (Poly-H) is then

$$d[\text{Poly-H}]/dt = k_3[\text{Poly-O}_2\cdot\,][\text{Poly-H}] \tag{6}$$

As we are assuming that steady-state conditions exist for [Poly-O_2 ·], then

$$\log[\text{Poly-H}] = -k_3[\text{Poly-O}_2\cdot\,]t/2.303 + \log[\text{Poly-H}]_0 \tag{7}$$

where $[\text{Poly-H}]_0 \equiv$ concentration of C—H moieties at some initial time.

If it is assumed that one molecule of a (C=O) containing compound is formed for every termination of two (Poly-O_2 ·) radicals, then

$$d[\text{C=O}]/dt = k_t[\text{Poly-O}_2\cdot\,]^2 \tag{8}$$

the solution of which yields

$$[\text{Poly-O}_2\cdot\,] = \left\{([\text{C=O}]-C_1)/k_t t\right\}^{1/2} \tag{9}$$

where $C_1 \equiv$ concentration of (C=O) at some initial time. Substitution of eq. (9) into eq. (7) provides the solution for the concentration [Poly-H], a relationship which is linear in $t^{1/2}$:

$$\log[\text{Poly-H}]/\left\{[\text{C=O}]-C_1\right\}^{1/2} = k_3 t^{1/2}/2.303 k_t^{1/2} + \log[\text{Poly-H}]_0/\left\{[\text{C=O}]-C_1\right\}^{1/2} \tag{10}$$

Measured concentrations of (Poly-H) and (C=O) were used to construct plots of eq. (10) for each of the aging conditions. Good linear behavior, as represented by Figure 4, was obtained except for the 40°C, 20% $[O_2]$ aging environment. These specimens apparently did not reach steady-state conditions during the course of the exposure. For the others, the ratios $k_3/k_t^{1/2}$ were found from the slopes of the straight line region of the plots.

If it is assumed that the rate of radical generation equals the rate of radical termination, then $k_t = k_i$. Chien et al.[8,9] developed an Arrhenius expression for k_i from a study of the decomposition of polymeric hydroperoxy radicals. A combination of their results with the slopes obtained from eqs. (10) yields Arrhenius plots for k_3. These are shown in Figures 5 and 6 for dry and wet aging conditions.

The steady-state rate equation for oxidation in FM-73U;

$$\rho_{ox} = k_2[\text{Poly}\cdot\,][O_2] = k_3[\text{Poly-O}_2\cdot\,][\text{Poly-H}] + k_t[\text{Poly-O}_2\cdot\,]^2 \tag{11}$$

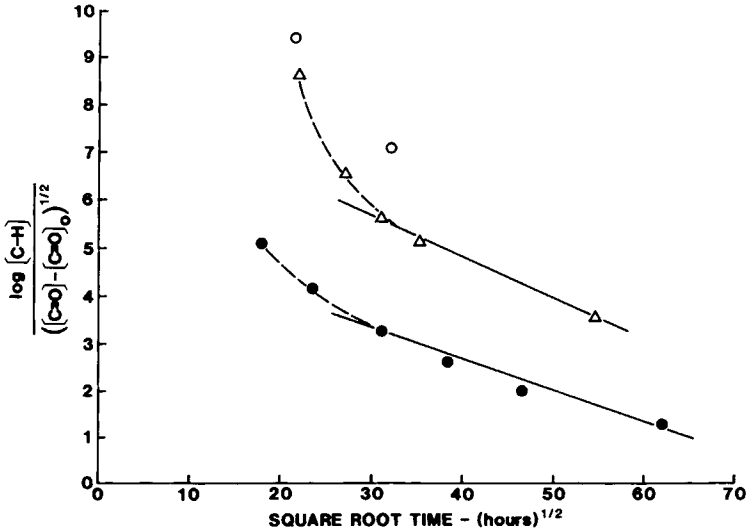

Fig. 4. Measured values of the dependent variable of eq. (11) as a function of time for FM-73U aged in 0% relative humidity, 20% oxygen environments. Aging temperature: (○) 40°C; (△) 50°C; (●) 60°C.

may be solved for ρ_{ox} at any of the exposure conditions by inserting the experimentally determined values of k_3 and [Poly-H] and the values of k_t from Chien et al.[8,9] It was found that at the partial pressures of O_2 used in these experiments ρ_{ox} was essentially independent of O_2 concentration. Therefore, ρ_{ox} is essentially first order in [Poly ·].

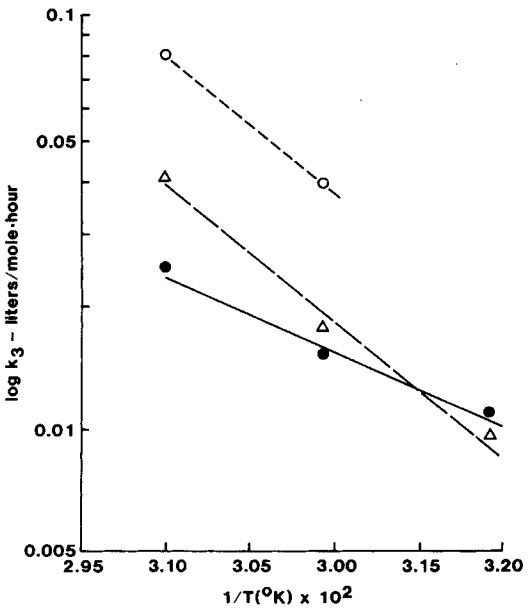

Fig. 5. Arrhenius plot of the rate constant k_3. The relative humidity during all exposures was 0%. Oxygen content: (○) 20%; (△) 40%; (●)) 100%.

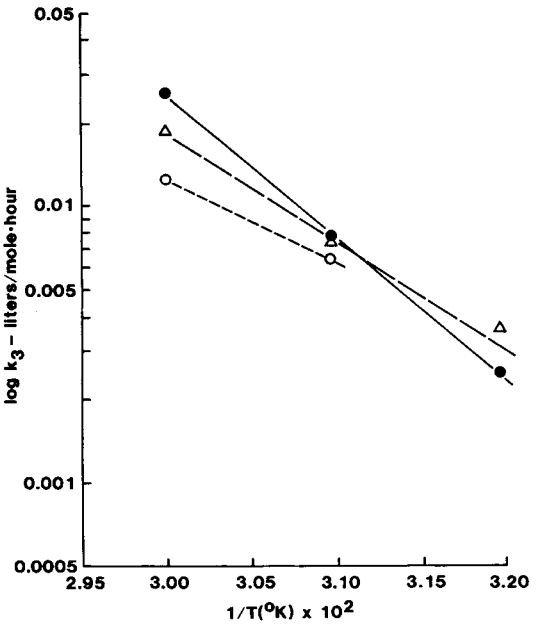

Fig. 6. Arrhenius plot of the rate constant k_3. The relative humidity during all exposures was 84%. Oxygen content: (○) 20%; (△) 40%; (●) 100%.

CYCLIC CRACK GROWTH MEASUREMENTS

Compact tension (CT) specimens were machined to size as specified by ASTM E647 from material plaques which had been cured according to vendor specification and cooled slowly to room temperature in order to minimize free volume. Cyclic crack growth rates were measured on specimens aged 0 weeks, 18 weeks, and 8 months in each of the environments listed in Table I.

Fatigue testing was done at room temperature on an Instron hydraulic servo machine with feedback control. Specimens, which had been aged in moist environments, were kept moist during testing. Each specimen was precracked and tested using a 1.0-Hz haver-triangle load wave form with a stress ratio maintained at $R = 0.1$.

Crack length during testing was determined by the crack opening displacement (COD) method.[10] Prior to extensive testing, a calibration was run on eight unaged CT specimens. This calibration established a correlation between COD, as measured by an extensometer located at the mouth of the crack, and crack length as measured by an optical comparator accurate to ± 1 mil. Crack lengths in subsequent tests were found from the measured COD, and the calibration curve was corrected for the modulus appropriate to each individual aging condition. These data were reduced to cyclic crack growth rates by the secant formula

$$(da/dN)_{a=\bar{a}} = (a_{i+1} - a_i)/(N_{i+1} - N_i) \tag{12}$$

where a_i is the length of the crack after N_i cycles of the load and

$$\bar{a} = (a_{i+1} + a_i)/2$$

The stress intensity factors were calculated from

$$\Delta K = \Delta P(2 + a/w)\, F(a/w)/Bw^{1/2}(1 - a/w)^{3/2} \tag{13}$$

where $F(a/w)$ is a fourth-order polynomial given by Ref. 10, a = crack length, w = specimen width, B = specimen thickness, and ΔP is the difference between the maximum and the minimum of the load cycle.

Plots of da/dN vs. ΔK were constructed from the crack growth measurements. Figure 7 is a typical example of the results. Note the slight curvature seen in the plotted data. Many of the other aging conditions yielded plots with similar curvature, suggesting that the lower stress intensities employed in the measurements were near the threshold for crack growth.

PREDICTION OF CRACK GROWTH RATES

Regression methods were applied to each plot to obtain values of the Paris parameters γ and C for each combination of age and exposure. These parameter values were then correlated with the degree of oxidation in each specimen as predicted by eq. (11).

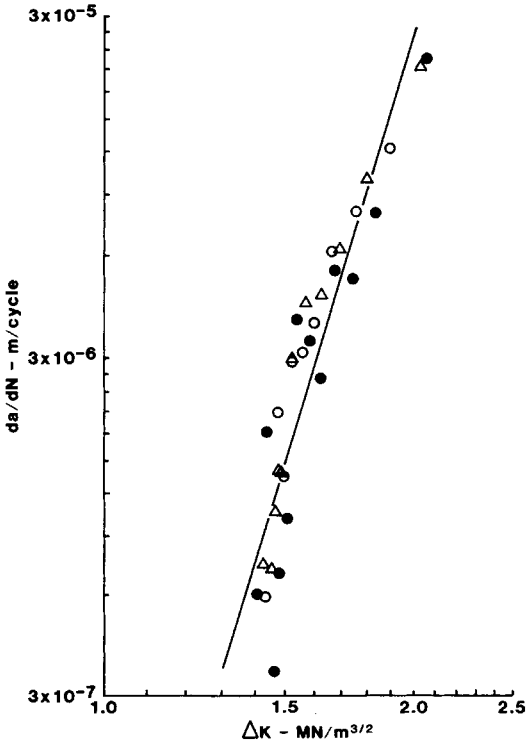

Fig. 7. Cyclic crack growth in FM-73U aged at 60°C for 8 months in 100% oxygen and 90% relative humidity. Data for three specimens are shown: (-) least squares fit to the data points.

The scatter plots shown in Figures 8 and 9 suggest that the Paris parameters are related to thermooxidative aging as measured by the oxidation index, $\rho_{ox} \cdot t$. Except for two points, there appears to be a reasonably good linear relationship between each Paris parameter and the oxidation index. Discernable differences between wet and dry exposures were not apparent. This was explicitly confirmed in fatigue tests on aged samples. It is seen that whereas the exponent γ increases with oxidation, the amplitude factor C decreases. Thus, the crack growth curves rotate counterclockwise as oxidation proceeds. This effect is illustrated in Figure 10, where the measured crack growth in unaged samples at room temperature and at 60°C are compared with the predicted crack growth in samples aged for 10 years in ambient conditions (room temperature, dry, 20% oxygen concentration). This prediction was calculated by first using eq. (11), with appropriate rate constants, to predict the oxidation index for 10 years of ambient aging; then the linear relationships of Figures 8 and 9 were used to obtain Paris parameters for use in eq. (1). It is seen that the material, as expected, becomes more brittle with age.

DISCUSSION

The oxidation index corresponding to the 10-year prediction of Figure 10 has a value of $\rho_{ox} \cdot t = 462$. This is somewhat greater than the largest oxidation index calculated for the specimens which were fatigue tested. Thus the prediction of Figure 10 involves a significant extrapolation of the linear behavior shown in Figures 8 and 9.

In addition, the role that diffusion plays in the oxidation process has not been fully considered. On the basis of autoxidation studies of poly-4-methylpenetene-1, Billingham and Walker[11] found a 3–8% deviation from a non-diffusion-controlled oxidation rate for specimens of thickness in the range 0.025–0.05 mm. Thus the oxidation of the FTIR specimens used in this work

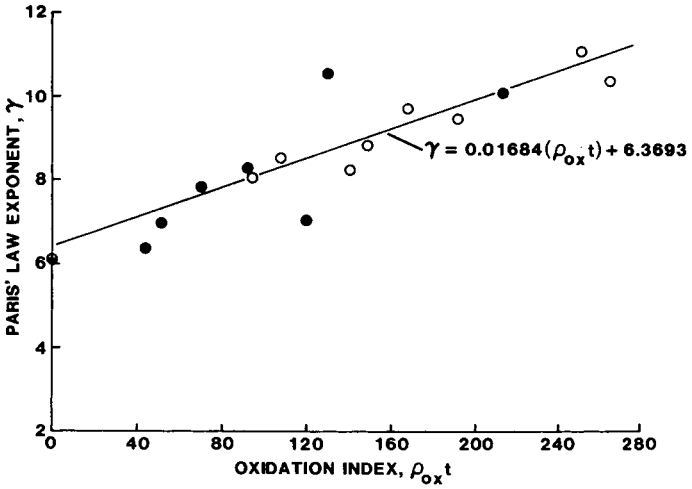

Fig. 8. Paris' law exponent γ vs. oxidation index $\rho_{ox}t$, where ρ_{ox} is the oxidation rate and t is the exposure time (h). Typical uncertainty in the plotted values of the exponent is ± 0.36. Relative humidity: (●) 0%; (○) 84%.

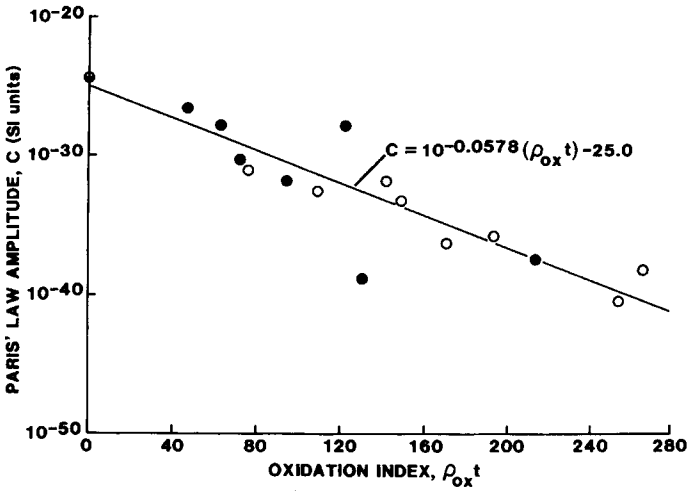

Fig. 9. Paris' law amplitude factor C vs. oxidation index $\rho_{ox}t$, where ρ_{ox} is the oxidation rate and t is the exposure time in hours. The ordinate is expressed in Standard International (SI) units. Typical uncertainty in the plotted values is ± 1.5 decades. Relative humidity: (●) 0%; (○) 84%.

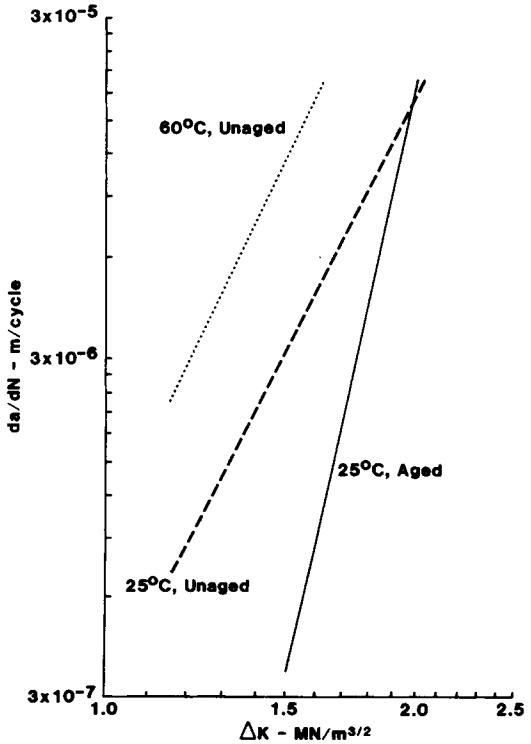

Fig. 10. Predicted crack growth rate (-) for FM-73U aged 10 years at 25°C, 0% relative humidity in a 20% oxygen environment. This is compared with measured crack growth rates for unaged FM-73U at 25°C (–) and 60°C (—), 0% relative humidity.

was probably not diffusion-limited. On the other hand, the much thicker fatigue specimens were likely not uniformly oxidized.

The aging characterization presented in this paper has focused on thermooxidation as a degradation mechanism of an adhesive. Extrapolations and simplifying assumptions were made in the interest of illustrating a prediction strategy and the potential impact of the aging process upon the service life of a bonded joint. More realistic investigations are called for. These should take into account the influence of joint geometry, adherend surface preparation, local stresses, and service profiles. Furthermore, other material aging mechanisms need to be considered. Physical aging, for example, has been shown to cause significant changes in the response properties of epoxy adhesives.[12] Shrinkage during and after cure, and gradual loss of plasticizers may produce similar effects.[13] Finally, although debonding is not a major cause of failure in a fresh, properly made joint, interfacial properties may change with age in ways that are not fully understood at this time. Thus, debonding may become a significant failure mode during the service lifetime of a bonded joint.

The authors wish to acknowledge the support of the Materials Laboratory of the Air Force, Wright Aeronautical Laboratories, Ohio, provided under Contract No. F33615-80-C-5093. We especially appreciate the guidance provided by Dr. W. B. Jones, project monitor.

References

1. P. C. Paris and F. Erdogan, *J. Basic Eng., ASME* Trans., *D*, **85**(4), 528 (1963).
2. J. A. Manson and L. H. Sperling, *Polymer Blends and Composites*, Plenum, New York, 1977, p. 102.
3. W. Althof, "The Diffusion of Water Vapor in Humid Air into the Bondlines of Adhesively Bonded Joints," 11th National SAMPE Technology Conference, Boston, November 13–15, 1979.
4. D. Katz and A. Buchman, *Polym. Eng. Sci.*, **171**, 85 (1971).
5. R. L. Pecsok, P. C. Painter, J. R. Shelton, and J. L. Koenig, *Rubber Chem. Technol.*, **49**, 1010 (1976).
6. S. C. Lin, B. J. Bulkin, and E. M. Pearce, *J. Polym. Sci.*, **17**, 3121 (1979).
7. S. W. Benson, *Thermochemical Kinetics*, Wiley, New York, 1968, p. 148.
8. J. C. W. Chien and H. Jablover, *J. Polym. Sci., Al*, **6**, 393 (1968).
9. J. C. W. Chien and H. Boss, *J. Polym. Sci., Al*, **5**, 3091 (1967).
10. J. Harrison, *Metal Constr.*, **12**, 415 (1980).
11. N. C. Billingham and T. J. Walker, *J. Polym. Sci., Polym. Chemi. Ed.*, **13**, 1209 (1975).
12. D. Hunston, W. Carter, and J. Rushford, "Linear Viscoelastic Properties of Solid Polymers as Modeled by a Simple Epoxy," in *Developments in Adhesives—2*, A. Kinloch, Ed., Elsevier, New York, 1984.
13. D. Peretz and Y. Weitsman, "Assessment of Chemical Cure-Shrinkage Effects on Residual Stresses in a Technical Adhesive," Mechanics and Materials Report No. 4089-81-8, Texas A & M University, 1981.

Received December 7, 1983
Accepted February 4, 1984
Corrected proofs received September 19, 1984